Targeting the cyclin-dependent kinase 5 in metastatic melanoma

Samanta Sharma[a,b], Tian Zhang[c], Wojciech Michowski[a,b], Vito W. Rebecca[d], Min Xiao[d], Roberta Ferretti[e,f], Jan M. Suski[a,b], Roderick T. Bronson[g], Joao A. Paulo[c], Dennie Frederick[h], Anne Fassl[a,b], Genevieve M. Boland[h], Yan Geng[a,b], Jacqueline A. Lees[e,i], Rene H. Medema[j], Meenhard Herlyn[d], Steven P. Gygi[c], and Piotr Sicinski[a,b,1]

[a]Department of Cancer Biology, Dana-Farber Cancer Institute, Boston, MA 02215; [b]Department of Genetics, Blavatnik Institute, Harvard Medical School, Boston, MA 02115; [c]Department of Cell Biology, Harvard Medical School, Boston, MA 02115; [d]Oncogenesis Program, The Wistar Institute, Philadelphia, PA 19104; [e]David H. Koch Institute for Integrative Cancer Research, Massachusetts Institute of Technology, Cambridge, MA 02139; [f]Translational Innovation Platform Oncology, Emmanuel Merck Darmstadt (EMD) Serono Research and Development Institute, Inc., Billerica, MA 01821; [g]Rodent Histopathology Core, Harvard Medical School, Boston, MA 02115; [h]Department of Surgery, Massachusetts General Hospital, Harvard Medical School, Boston, MA 02114; [i]Department of Biology, Massachusetts Institute of Technology, Cambridge, MA 02139; and [j]Division of Cell Biology, Oncode Institute, Netherlands Cancer Institute, 1066 CX Amsterdam, The Netherlands

Edited by Richard Marais, Cancer Research UK Manchester Institute, Macclesfield, United Kingdom, and accepted by Editorial Board Member Anton Berns February 10, 2020 (received for review July 22, 2019)

The cyclin-dependent kinase 5 (CDK5), originally described as a neuronal-specific kinase, is also frequently activated in human cancers. Using conditional CDK5 knockout mice and a mouse model of highly metastatic melanoma, we found that CDK5 is dispensable for the growth of primary tumors. However, we observed that ablation of CDK5 completely abrogated the metastasis, revealing that CDK5 is essential for the metastatic spread. In mouse and human melanoma cells CDK5 promotes cell invasiveness by directly phosphorylating an intermediate filament protein, vimentin, thereby inhibiting assembly of vimentin filaments. Chemical inhibition of CDK5 blocks the metastatic spread of patient-derived melanomas in patient-derived xenograft (PDX) mouse models. Hence, inhibition of CDK5 might represent a very potent therapeutic strategy to impede the metastatic dissemination of malignant cells.

cyclin-dependent kinases | CDK5 | metastasis | mouse cancer models

Cyclin-dependent kinases (CDKs) represent a family of proline-directed serine/threonine kinases that are activated by the interaction with different cyclin proteins. Individual cyclin-CDK complexes become activated at specific points of cell cycle progression and phosphorylate several cellular proteins, thereby driving cell division (1, 2). Abnormally elevated activity of cyclin-CDK complexes, especially cyclin D-CDK4, D-CDK6, and E-CDK2, represents the driving force of unconstrained cell proliferation in a large fraction of human tumors (3). Inhibitors of cyclin-dependent kinases, in particular compounds that target CDK4 and CDK6, have been recently approved for treatment of breast cancers and are in clinical trials for several other cancer types (4). Consistent with the growth-promoting function of these cell cycle CDKs, their inhibition results in growth arrest of cancer cells (4, 5). Unfortunately, targeting cell cycle CDKs has not been shown to impede other aspects of tumorigenesis, such as the ability of cancer cells to form lethal metastases.

Cyclin dependent kinase 5 (CDK5) represents an unusual CDK. Unlike other CDKs, this kinase is not activated by interaction with cyclin proteins. Instead, CDK5 becomes active upon binding to noncyclin p35 and p39 proteins (6). Moreover, in contrast to other CDKs which require an activating phosphorylation on Thr-160 (carried out by the CDK-activating kinase [CAK]), physical interaction with p35/p39 proteins is sufficient to fully activate CDK5 (6).

CDK5 is ubiquitously expressed; however, its activators p35 and p39 are mainly expressed in the nervous system, resulting in neuronal-specific activation of CDK5 (6). During development of the nervous system, CDK5 becomes active once the neuronal progenitors have exited the cell cycle, and it is maintained in the postmitotic neurons (7). CDK5-p35/p39 kinases were shown to regulate a wide range of neuronal functions, including synapse formation and plasticity, axon guidance, neurite outgrowth, membrane transport, and neuronal migration, through phosphorylation of various neuronal substrates (6, 8).

Growing evidence indicates that CDK5 is also active in human cancer cells. Several studies documented that human cancers express CDK5 and p35 and contain catalytically active CDK5-p35 complexes. Moreover, high expression of CDK5 and p35 in tumor cells confers overall poor prognosis (9–13).

The function of CDK5 in cancer cells remains unclear. Since no CDK5-specific inhibitors are available, most studies employed pan-CDK inhibitors, or dominant-negative CDK5 constructs, or anti-CDK5 shRNAs. These studies led to some conflicting results which implicated CDK5 in promoting or inhibiting tumor cell proliferation, stimulating or impeding cell motility, or survival, or angiogenesis (14) (see *Discussion*).

In the current study, we decided to dissect the function of CDK5 in tumorigenesis using genetic means, namely conditional CDK5 knockout (KO) mice and a mouse model of melanoma. Moreover, to selectively inhibit CDK5 in tumor cells, we engineered

Significance

Melanomas are notorious due to their propensity to form lethal metastases. Currently, no treatments are available to stop the metastatic spread. We observed that in malignant melanomas, a protein called the cyclin-dependent kinase 5 (CDK5) is essential for melanoma metastasis. Using mouse and human melanoma cells, we demonstrated that in this tumor type CDK5 promotes the metastatic spread by directly phosphorylating a mesenchymal-type intermediate filament, vimentin. We found that a genetic shutdown of CDK5 in a mouse model of melanoma abrogated metastasis, while chemical inhibition of CDK5 kinase in mice carrying patient-derived tumors impeded the metastatic spread of tumor cells. Our results indicate that inhibition of CDK5 might represent a therapeutic strategy to block the metastatic dissemination of melanoma cells.

Author contributions: S.S., W.M., and P.S. designed research; S.S., T.Z., W.M., V.W.R., M.X., J.M.S., A.F., Y.G., and P.S. performed research; R.F., J.A.P., D.F., G.M.B., and J.A.L. contributed new reagents/analytic tools; S.S., R.T.B., Y.G., R.H.M., M.H., S.P.G., and P.S. analyzed data; and S.S. and P.S. wrote the paper.

Competing interest statement: P.S. has been a consultant at Novartis, Genovis, Guidepoint, The Planning Shop, ORIC Pharmaceuticals, and Exo Therapeutics; his laboratory receives research funding from Novartis. W.M. is currently an employee of Cedilla Therapeutics.

This article is a PNAS Direct Submission. R.M. is a guest editor invited by the Editorial Board.

[1]To whom correspondence may be addressed. Email: peter_sicinski@dfci.harvard.edu.

This article contains supporting information online at https://www.pnas.org/lookup/suppl/doi:10.1073/pnas.1912617117/-/DCSupplemental.

First published March 19, 2020.

mouse and human melanoma cells to express analog-sensitive CDK5. We report that CDK5 kinase is dispensable for melanoma cell proliferation, but it is essential for the metastatic spread. We observed that ablation of CDK5 abrogated formation of metastases in a highly metastatic mouse melanoma model. We also found that inhibition of CDK5 kinase blocked the metastatic spread of patient-derived melanomas in patient-derived xenograft (PDX) mouse models. We propose that inhibition of CDK5 might represent a very potent therapeutic strategy to impede the metastatic dissemination of malignant cells.

Results

Human Melanomas Express High Levels of CDK5. We began our analyses by comparing the expression levels of CDK5 transcripts across over 1,000 human cancer cell lines annotated in the Cancer Cell Line Encyclopedia. We observed that among cell lines representing different human tumor types, melanoma cell lines express the highest levels of CDK5 (*SI Appendix*, Fig. S1 *A* and *B*). A substantial proportion (over 50%) of melanoma cell lines displayed amplification of the *CDK5* locus (*SI Appendix*, Fig. S1*C*); we observed a correlation between the *CDK5* gene copy number and the levels of CDK5 transcripts (*SI Appendix*, Fig. S1*D*). Using Western blotting, we confirmed high levels of CDK5 protein in a panel of 10 human melanoma cell lines (*SI Appendix*, Fig. S1 *E* and *F*). We next analyzed CDK5 transcript levels among different types of human tumors annotated in cBioPortal Cancer Genomics (The Cancer Genome Atlas [TCGA] datasets). Again, we observed that CDK5 was expressed at particularly high levels in melanomas, as compared to several other tumor types (*SI Appendix*, Fig. S1 *G* and *H*). Moreover, analysis of TCGA revealed that alterations of CDK5 in melanomas (mostly gene amplification or transcript overexpression) correlate with poor prognosis (*SI Appendix*, Fig. S1*I*). Therefore, in our study we focused on the function of CDK5 in this tumor type.

Ablation of CDK5 Blocks the Metastatic Spread of Autochthonous Melanoma Tumors. To test the impact of CDK5 ablation on autochthonous tumors in vivo, we took advantage of a well-established Tyr-Cre/BRAF$^{V600E/+}$/PTEN$^{F/F}$ mouse model of melanoma. In these mice, the expression of an oncogenically activated *BRAF^{V600E}* allele and homozygous deletion of the *PTEN* gene are targeted to skin melanocytes by tamoxifen-inducible Cre recombinase, which is driven by the melanocyte-specific tyrosinase promoter (15). Topical administration of 4-hydroxytamoxifen (4-HT) onto the skin of Tyr-Cre/BRAF$^{V600E/+}$PTEN$^{F/F}$ mice turns on BRAF^{V600E} expression and ablates expression of PTEN (Fig. 1*A*). As a consequence, mice develop malignant and highly metastatic melanomas that rapidly spread to the internal organs (15, 16). The genetic lesions seen in Tyr-Cre/BRAF$^{V600E/+}$/PTEN$^{F/F}$ mice closely mimic those seen in human tumors. Thus, ∼65% of human melanomas contain point mutations within the *BRAF* gene that give rise to a constitutively active *BRAF^{V600E}* allele, while almost all tumors undergo silencing of the *PTEN* or *CDKN2A* genes (17–19). Importantly, we verified that melanomas arising in Tyr-Cre/BRAF$^{V600E/+}$/PTEN$^{F/F}$ mice express high levels of CDK5 and p35 proteins (Fig. 1*B*).

We crossed Tyr-Cre/BRAF$^{V600E/+}$/PTEN$^{F/F}$ mice with conditional knockout CDK5$^{F/F}$ mice (20) and generated CDK5$^{F/F}$/Tyr-Cre/BRAF$^{V600E/+}$/PTEN$^{F/F}$ animals. Administration of 4-HT to these mice is expected to delete the *CDK5* gene, concomitant with activation of BRAF^{V600E} and ablation of PTEN expression, thereby rendering melanocytes and the resulting tumors CDK5-null (Fig. 1*A*).

We applied 4-HT onto the skin of CDK5$^{F/F}$/Tyr Cre/BRAF$^{V600E/+}$/PTEN$^{F/F}$ and control CDK5$^{+/+}$/Tyr Cre/BRAF$^{V600E/+}$/PTEN$^{F/F}$ mice and observed the animals for tumor development. We found that CDK5$^{+/+}$ and CDK5$^{F/F}$ mice developed skin melanomas with identical kinetics. We verified by immunostaining of tumor sections with an anti-CDK5 antibody as well as by immunoblotting of tumor lysates that—as expected—tumors arising in CDK5$^{F/F}$ animals lost CDK5 expression (Fig. 1 *C* and *D* and *SI Appendix*, Fig. S2). In contrast, melanomas in CDK5$^{+/+}$ animals expressed high levels of CDK5 protein (Fig. 1 *C* and *D* and *SI Appendix*, Fig. S2). The mean number of tumors per mouse, the size of tumors, as well as the overall tumor burden were essentially identical in CDK5$^{+/+}$ and CDK5$^{F/F}$ animals (Fig. 1 *E* and *F*). Consistent with these findings, CDK5-deleted tumors displayed unperturbed fractions of 5-bromo-2′-deoxyuridine (BrdU)- and Ki-67–positive cells, as compared to CDK5$^{+/+}$ tumors (Fig. 1 *G* and *H*). We concluded that CDK5 is not required for the oncogenic transformation by the oncogenic BRAF and PTEN loss, and it is dispensable for the growth of primary tumors.

In the next set of experiments, we euthanized mice 35 d after administration of 4-HT and systematically analyzed their internal organs for the presence of macroscopic and microscopic metastases; the latter were verified by immunostaining of histological sections with antibodies against S100, a marker of melanocytes and melanoma cells (21). As expected, 8/10 of CDK5$^{+/+}$ animals displayed numerous distant metastases in the lungs and spleens. In contrast, 10/11 CDK5$^{F/F}$ animals were completely free of metastases (Fig. 2 *A* and *B*). In one CDK5$^{F/F}$ mouse, we detected the presence of a microscopic metastatic lesion in the spleen (Fig. 2*C*). Strikingly, immunostaining for CDK5 revealed that this lesion was entirely composed of CDK5-positive cells (Fig. 2*C*), indicating that the metastasis originated from a very small number of cells within the primary tumor that failed to delete CDK5 upon Cre expression (*SI Appendix*, Fig. S2).

An additional cohort of mice was observed until the animals became moribund, or their skin tumors reached the allowable size limit. All CDK5$^{+/+}$ mice had to be euthanized within 40 d after 4-HT administration. Necropsy and histopathological analyses revealed massive metastases in the internal organs in the majority of these animals. In contrast, the majority (8/10) of CDK5$^{F/F}$ animals, euthanized by day 60, were completely free of metastases (Fig. 2 *A* and *D*). In two CDK5$^{F/F}$ animals, we observed small metastatic lesions in the spleen. As before, we found that these metastases expressed CDK5, indicating that they arose from nondeleted cells in the primary tumor. Collectively, these observations indicate that CDK5 is not required for primary tumor formation and growth, but it plays an essential role in melanoma metastasis.

CDK5 Kinase Activity Is Required for Melanoma Cell Extravasation. To start dissecting the function of CDK5 in the metastatic spread, we employed in vivo metastasis assays (22, 23). In this approach, injection of highly metastatic mouse melanoma B16-F10 cells into the tail veins of recipient mice leads to formation of multiple lung metastases (Fig. 3*A*). We used CRISPR/Cas9 to knock out the *CDK5* gene in B16-F10 cells (Fig. 3*B* and *SI Appendix*, Fig. S3*A*). We next injected CDK5$^{+/+}$ and CDK5-KO cells into tail veins of C57BL/6 wild-type mice, and euthanized the animals after 3 and 4 wk. As expected, all mice inoculated with CDK5$^{+/+}$ melanoma cells became moribund and displayed lungs laden with metastatic tumors (Fig. 3 *C* and *D* and *SI Appendix*, Fig. S3*B*). In contrast, mice injected with CDK5-KO cells remained healthy and displayed only single metastatic lesions (Fig. 3 *C* and *D* and *SI Appendix*, Fig. S3*B*). Importantly, immunostaining with anti-CDK5 antibodies revealed that lung metastases found in mice injected with CDK5-KO cells expressed high levels of CDK5 protein (Fig. 3*E*). This indicates that, as we observed in the case of autochthonous tumors, the metastatic lesions arose from cells that escaped CRISPR-mediated ablation of CDK5. Another cohort of mice was observed for survival. All mice injected with CDK5$^{+/+}$ cells became moribund and had to be euthanized within 30 to 40 d. In contrast, a substantial fraction of mice inoculated with CDK5-KO melanoma cells remained healthy and tumor-free during the entire 300-d observation period (Fig. 3*F*).

It has been reported that CDK5 maintains expression of the programmed cell death ligand 1 (PD-L1) protein in tumor cells, which suppresses the immune response of the hosts (24). For this reason, we considered the possibility that the inability of CDK5-null cells to form metastases might be caused by elimination of

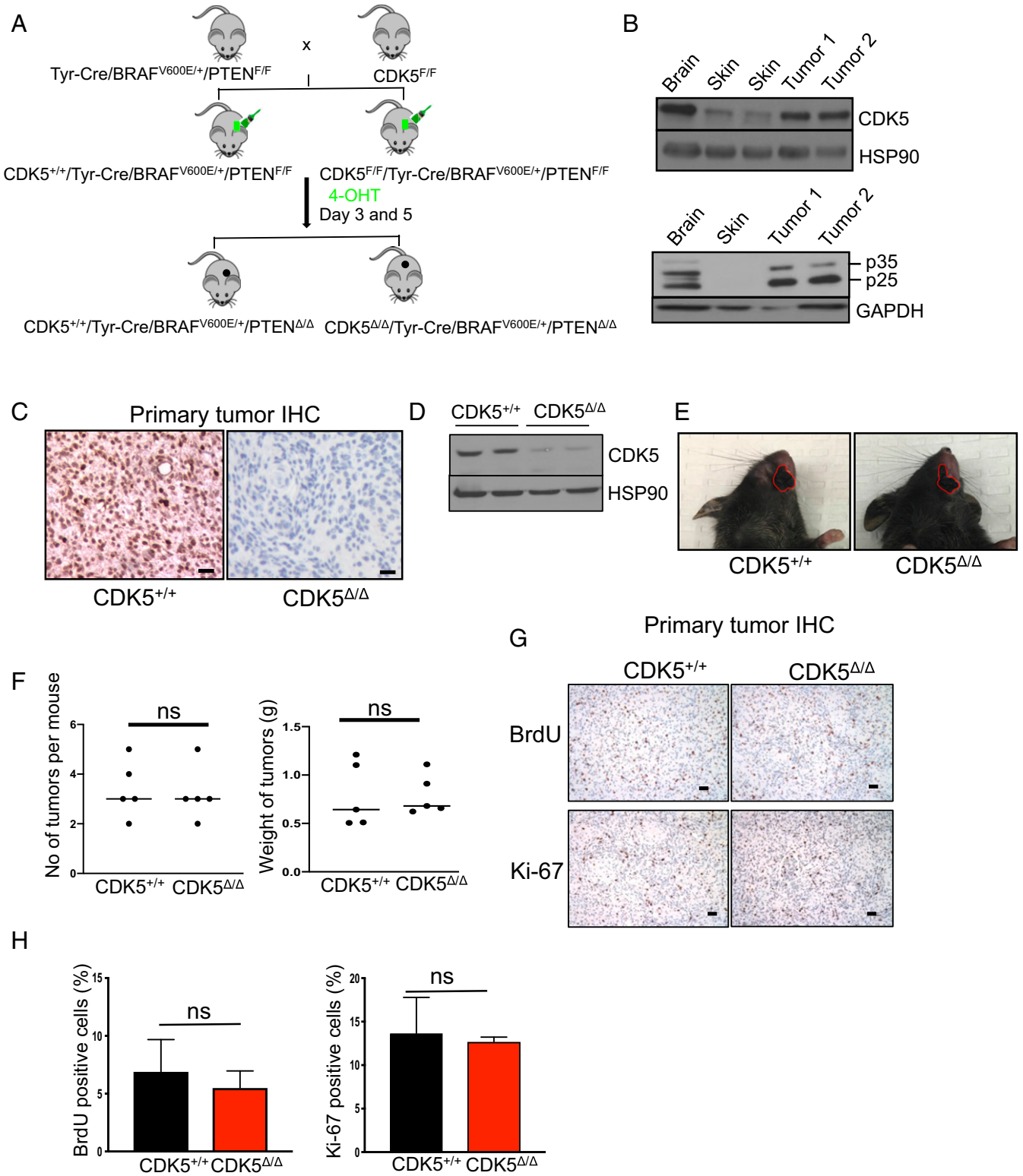

Fig. 1. Analyses of mouse melanoma tumors. (*A*) Schematic representation of the crosses to generate mice bearing CDK5$^{+/+}$/Tyr-Cre/BRAF$^{V600E/+}$/PTEN$^{\Delta/\Delta}$ and CDK5$^{\Delta/\Delta}$/Tyr-Cre/BRAF$^{V600E/+}$/PTEN$^{\Delta/\Delta}$ tumors. (*B*) Immunoblotting of tumor lysates for CDK5 (*Upper*) and p35 (*Lower*). p25 denotes proteolytically cleaved p35 species. Adjacent normal skin and brain (the latter as a positive control) were also analyzed. Immunoblotting for HSP90 and GAPDH was used as a loading control ($n = 2$). (*C*) Immunohistochemistry (IHC) staining of tumor sections with an anti-CDK5 antibody. (Scale bars, 50 μm.) (*D*) Immunoblotting of tumor lysates for CDK5 and HSP90 (loading control) ($n = 3$). (*E*) Examples of skin tumors (denoted by red contours) arising in CDK5$^{+/+}$ and CDK5$^{F/F}$ mice. (*F*) Quantification of the number of tumors per mouse and total tumor weight per mouse in CDK5$^{+/+}$ and CDK5$^{F/F}$ animals ($n = 5$ mice/group). ns, not significant; unpaired *t* test. (*G*) IHC staining of tumors for BrdU (*Upper*), or Ki-67 (*Lower*) to mark proliferating cells. (*H*) Quantification of the fractions of BrdU- or Ki-67–positive cells in CDK5$^{+/+}$ and CDK5$^{\Delta/\Delta}$ tumors ($n = 5$ mice/group). Shown are mean values ± SD (*Right*, unpaired *t* test; *Left*, unpaired *t* test with Welch's correction).

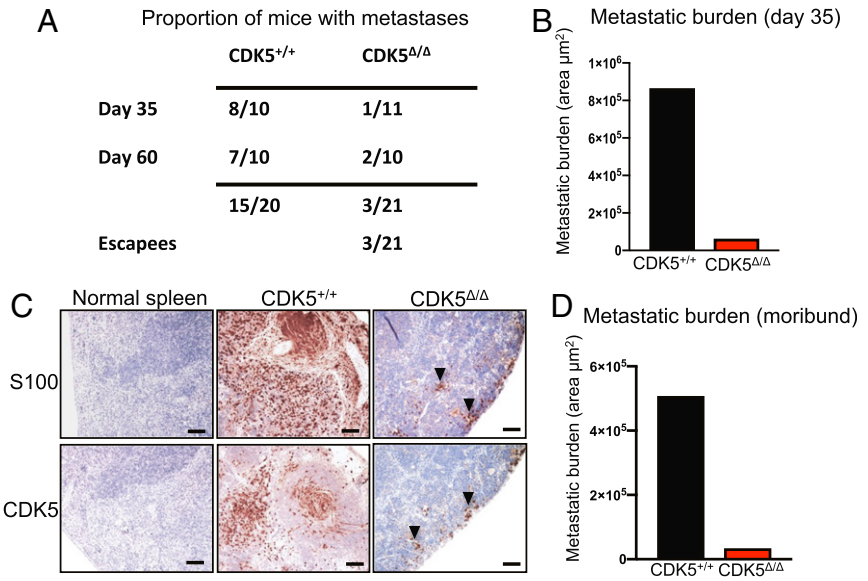

Fig. 2. CDK5 is essential for the metastatic spread. (*A*) Table showing the proportion of CDK5$^{+/+}$/Tyr-Cre/BRAF$^{V600E/+}$/PTEN$^{F/F}$ (CDK5$^{+/+}$) and CDK5$^{F/F}$/Tyr-Cre/BRAF$^{V600E/+}$/PTEN$^{F/F}$ (CDK5$^{\Delta/\Delta}$) animals displaying macroscopic or microscopic metastases in distal organs. $P < 0.05$ (Fisher's exact test). (*B*) Quantification of the total metastatic burden in the internal organs of CDK5$^{+/+}$/Tyr-Cre/BRAF$^{V600E/+}$/PTEN$^{F/F}$ (CDK5$^{+/+}$) and CDK5$^{F/F}$/Tyr-Cre/BRAF$^{V600E/+}$/PTEN$^{F/F}$ (CDK5$^{\Delta/\Delta}$) animals, euthanized on day 35. To estimate total metastatic burden in a given animal, we calculated the total area occupied by metastases in step sections of internal organs (*SI Appendix, Materials and Methods*). (*C*) Immunostaining of spleen sections from a control mouse (normal spleen), or spleens with metastases from CDK5$^{+/+}$/Tyr-Cre/BRAF$^{V600E/+}$/PTEN$^{F/F}$ (CDK5$^{+/+}$) or CDK5$^{F/F}$/Tyr-Cre/BRAF$^{V600E/+}$/PTEN$^{F/F}$ (CDK5$^{\Delta/\Delta}$) mice. Sections were immunostained for S100 (a marker of melanocytes and melanoma cells) or CDK5, and counterstained with hematoxylin. Note that small clusters of metastatic cells in a CDK5$^{F/F}$/Tyr-Cre/BRAF$^{V600E/+}$/PTEN$^{F/F}$ mouse were CDK5-positive (arrowheads), indicating that they arose from cells that escaped CDK5 deletion (*SI Appendix*, Fig. S2). (Scale bars, 50 μm.) (*D*) Quantification of the total metastatic burden in the internal organs of CDK5$^{+/+}$/Tyr-Cre/BRAF$^{V600E/+}$/PTEN$^{F/F}$ (CDK5$^{+/+}$) and CDK5$^{F/F}$/Tyr-Cre/BRAF$^{V600E/+}$/PTEN$^{F/F}$ (CDK5$^{\Delta/\Delta}$) animals, euthanized when the tumor sizes reached allowable limit, or the animals became moribund or paralyzed (by day 40 in CDK5$^{+/+}$ and day 60 in CDK5$^{F/F}$ mice). Total metastatic burden was estimated as in *B*.

these cells by the host immune system. To test this possibility, we repeated in vivo metastasis assays using immunodeficient nude (*Foxn1^{nu}*) mice as recipients. We found that also in these immunodeficient mice, CDK5-null cells failed to efficiently form lung metastases (Fig. 3*G*). These observations indicate that the inability of CDK5-null cells to metastasize is not due to their elimination by the immune system.

We next asked whether the requirement for CDK5 function in the metastatic spread depends on CDK5 kinase activity. This issue could not have been conclusively resolved before due to the lack of CDK5-specific inhibitors. To overcome this limitation, we generated an analog-sensitive (*as*) version of CDK5. To generate an *as* kinase, the large hydrophobic "gatekeeper" residue in the kinase ATP-binding pocket is mutated from the naturally occurring "bulky" residue to glycine or alanine. This creates an enlarged pocket not found in any wild-type kinase (25) (Fig. 4*A*). Numerous studies demonstrated that the *as* substitution does not alter substrate specificity of the kinases (26–28). However, the engineered *as* kinase can be uniquely inhibited by compounds that occupy the enlarged ATP-binding pocket, such as 1-NM-PP1, 1-NA-PP1, or 3-MB-PP1 (Fig. 4*A*). Importantly, *as* inhibitors do not inhibit any wild-type kinases in the mammalian kinome (25, 29). Hence, by treating cells expressing an *as* kinase with *as* inhibitors one can selectively shut down the activity of this kinase (29).

We engineered *as*CDK5 protein by mutating the bulky gatekeeper residue in the CDK5 ATP-binding pocket from phenylalanine 80 to a smaller amino acid, glycine. We first verified that *as*CDK5 can be potently inhibited by 1-NM-PP1 (Fig. 4*B*). As expected, 1-NM-PP1 had no effect on the kinase activity of wild-type CDK5 (Fig. 4*B*). We next knocked out CDK5 in mouse melanoma B16-F10 cells and ectopically expressed analog-sensitive CDK5, thereby generating *as*CDK5 cells (Fig. 4*C*).

To test whether the kinase activity of CDK5 is required for the metastatic spread, we injected B16-F10 cells expressing *as*CDK5 into tail veins of C57BL/6 mice. The recipient mice were continuously treated with 1-NA-PP1 (to inhibit CDK5 in tumor cells), or with vehicle (control) and euthanized after 3 wk. As expected, mice treated with vehicle developed numerous lung metastases. In contrast, the number of metastases was dramatically reduced in mice treated with 1-NA-PP1 (Fig. 4*D* and *SI Appendix*, Fig. S3*C*). These observations indicated that CDK5 kinase activity is required for metastatic dissemination of melanoma cells.

To further define the stage of the metastatic spread at which CDK5 kinase plays a rate-limiting role, we labeled *as*CDK5 B16-F10 cells with fluorescent CellTracker Orange CMRA dye, and injected them into tail veins of *Foxn1^{nu}* mice. We previously established that in this approach, the extravasation of melanoma cells is completed within 1 to 2 d (23). The recipient mice were continuously treated with an inhibitor of *as* kinases or with vehicle (control), and their lungs were imaged at different time points to evaluate the presence of fluorescent tumor cells. We observed that after 2 h, similar numbers of tumor cells were present in the lungs of inhibitor-treated and control mice, indicating a similar degree of capillary entrapment (Fig. 4 *E*, *Left*). In contrast, the number of tumor cells retained in the lungs after 1 or 2 d was strongly reduced in recipient mice receiving the inhibitor (Fig. 4 *E*, *Right*). Similar results were obtained using CDK5-knockout B16-F10 cells (*SI Appendix*, Fig. S3 *D* and *E*). These observations suggested that CDK5 kinase activity is required during early stages of the metastatic spread, when tumor cell extravasation takes place.

We next investigated the consequences of CDK5 inhibition after the extravasation had been completed. To this end, we injected *as*CDK5 B16-F10 cells into tail veins of recipient mice and started treatment with an inhibitor of *as* kinases after 2 d, i.e., the time point when tumor cells have exited the capillaries and entered the lung parenchyma (23). Mice were continuously treated for 4 wk, euthanized, and their lungs evaluated for the presence of metastases. We observed that when started at 2 d postinjection, CDK5 inhibition had no effect on the ability of cells to form lung tumors (*SI Appendix*, Fig. S3*F*). These results suggest that during the metastatic spread, CDK5 kinase is essential only during the initial colonization of the lung parenchyma, but it is dispensable at later stages.

To further confirm these observations and to extend them to human melanomas, we depleted CDK5 in 10 in vitro cultured human melanoma cell lines. We next subjected these cells to in vitro Transwell invasion assays (23). We observed that depletion of CDK5 reduced in vitro invasiveness in 9/10 cell lines (*SI Appendix*, Fig. S3 *G* and *H*).

We next engineered human melanoma A-375 cells to express *as*CDK5 in place of wild-type CDK5, using the same approach as

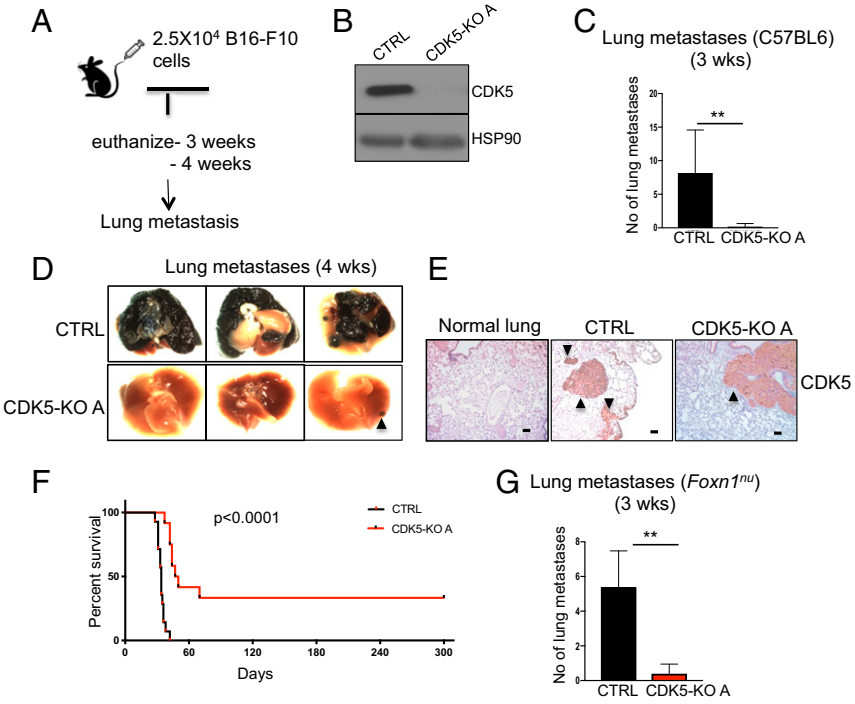

Fig. 3. In vivo metastasis assays. (*A*) Schematic representation of the experimental approach to generate lung metastases. (*B*) Immunoblotting of $CDK5^{+/+}$ (CTRL) and CDK5-knockout (CDK5-KO A) mouse melanoma B16-F10 cells for CDK5 and HSP90 (loading control) ($n = 3$). (*C*) The numbers of lung metastases in C57BL/6 mice injected with $CDK5^{+/+}$ (CTRL) or CDK5-KO melanoma cells, quantified after 3 wk ($n = 5$ mice/group). Shown are mean values ± SD $^{**}P < 0.01$ (Mann–Whitney *U* test). (*D*) The appearance of lungs from animals as above, 4 wk after injection of melanoma cells ($n = 5$ mice/group). An arrowhead points to a metastatic lesion in a mouse injected with CDK5-KO cells. (*E*) Sections of lungs from a healthy normal animal (normal lung), or from animals injected with $CDK5^{+/+}$ (CTRL), or CDK5-KO melanoma cells were immunostained for CDK5 ($n = 5$ mice/group). Note that a metastatic lesion found in a mouse injected with CDK5-KO cells was CDK5-positive, indicating that it arose from cells that escaped CDK5 deletion. Metastatic tumors are marked by arrowheads. (Scale bars, 50 μm.) (*F*) Survival curves of mice injected with $CDK5^{+/+}$ (CTRL) or CDK5-KO melanoma cells ($n = 10$ mice/group). $P < 0.0001$ (Log-rank test). (*G*) The numbers of lung metastases in immunocompromised $Foxn1^{nu}$ mice injected with $CDK5^{+/+}$ (CTRL) or CDK5-KO melanoma cells, quantified after 3 wk ($n = 5$ mice/group). Shown are mean values ± SD $^{**}P < 0.01$ (Mann–Whitney *U* test).

the one employed to generate *as*CDK5 mouse melanoma B16-F10 cells (Fig. 4*F*). We cultured *as*CDK5 mouse and human melanoma cells in the presence of 3-MB-PP1 and evaluated the impact on cell invasiveness. We observed that inhibition of CDK5 essentially phenocopied CDK5 ablation, namely it impeded the invasiveness of melanoma cells (Fig. 4 *G* and *H*).

During the metastatic spread, malignant cells must be able to invade through the endothelial cell layer. Our in vivo observations and in vitro invasion assays suggested that this step of melanoma cell dissemination might be impaired in CDK5-inhibited and CDK5-null cells. To further evaluate the impact of CDK5 inhibition on this process, we subjected cells to in vitro transendothelial migration assays (also known as in vitro extravasation assays) (23). Melanoma cells were seeded on top of human umbilical vein endothelial cell (HUVEC) monolayers, and tumor cells reaching the lower side of the membrane were quantified over time. Consistent with our in vivo observations, we found that knockout of CDK5, or an acute inhibition of CDK5 kinase impaired the ability of mouse and human melanoma cells to undergo transendothelial migration (Fig. 4 *I* and *J* and *SI Appendix*, Fig. S3 *I–K*). Collectively, these observations suggest that CDK5 likely plays a rate-limiting role in extravasation of melanoma cells, as inhibition of CDK5 kinase impeded this process in vitro and in vivo. In addition, plating of melanoma cells onto collagen- and fibronectin-coated surfaces revealed a mild impairment of adhesion in CDK5-null cells (*SI Appendix*, Fig. S4 *A–C*). It is possible that these mild defects also contribute to the impeded invasiveness and extravasation of CDK5-deficient cells.

In order to further characterize the impact of CDK5 deficiency or CDK5 kinase inhibition on other properties of melanoma cells, we subjected mouse B16-F10 and human A-375 melanoma cells to additional assays. Since the ability of cells to evade apoptosis due to nutrient deprivation plays an important role in metastasis (30), we evaluated the response of CDK5-null cells to culturing them in serum-free medium. We observed no differences between the apoptotic rate of CDK5-proficients vs. CDK5-deficient cells (*SI Appendix*, Fig. S4 *D* and *E*). Another important property of metastatic cells is the ability to survive in suspension and to evade anoikis (30). To gauge this, cells were detached from substratum, kept in suspension, and cell survival was monitored over time. Again, no differences were detected between parental and CDK5 knockout cells (*SI Appendix*, Fig. S4 *F* and *G*). Collectively, these observations suggested that the defects in tumor cell invasiveness and extravasation, demonstrated above, likely underlie the inability of CDK5-deficient cells to form metastases.

CDK5 Directly Phosphorylates Vimentin and Regulates Vimentin Polymerization in Melanoma Cells. To understand the molecular function played by CDK5 kinase in melanoma metastasis, we wished to identify melanoma proteins that critically depend on CDK5 for their phosphorylation. To do so, we inhibited CDK5 by treating in vitro cultured *as*CDK5 B16-F10 melanoma cells with 3-MB-PP1. Subsequently, we prepared lysates from CDK5-inhibited and control (vehicle treated) cells, labeled the peptides from the two conditions with different isobaric tandem mass tags (TMTs) (31, 32), enriched for phosphorylated peptides, and performed total phosphoproteome profiling using quantitative mass spectrometry. Inhibition of CDK5 resulted in decreased phosphorylation (≥1.5 fold decrease, $P < 0.01$) of 22 phosphopeptides belonging to 13 proteins (Dataset S1C). Among them, the most strongly decreased (over 8.8-fold) was phosphorylation of vimentin protein at serine 56 (Fig. 5*A*, *SI Appendix*, Fig. S5*A*, and Dataset S1).

Vimentin, an intermediate filament protein found in mesenchymal cells, has been demonstrated to play an essential role in regulating the motility and invasiveness of cancer cells, including melanomas (33–36). Importantly, serine 56 residue of vimentin was shown to be phosphorylated during mitosis by a cell cycle kinase CDK1, which is closely related (58% amino acid identity) to CDK5 (37). Phosphorylation of serine 56 during mitosis triggers disassembly (depolymerization) of vimentin filaments prior to cell division (38, 39). In addition to CDK1, other kinases, such as PKA and PKC can phosphorylate vimentin in interphase cells, and this also triggers depolymerization of vimentin filaments (40–43). Importantly, disassembly of vimentin filaments is required for cell migration, while filament stabilization impedes this process (36, 40). Hence, we hypothesized that in melanoma cells, CDK5 might directly regulate the depolymerization of vimentin filaments, thereby promoting cell migration.

To test this hypothesis, we first confirmed that vimentin represents a direct phosphorylation substrate of CDK5 in intact cells

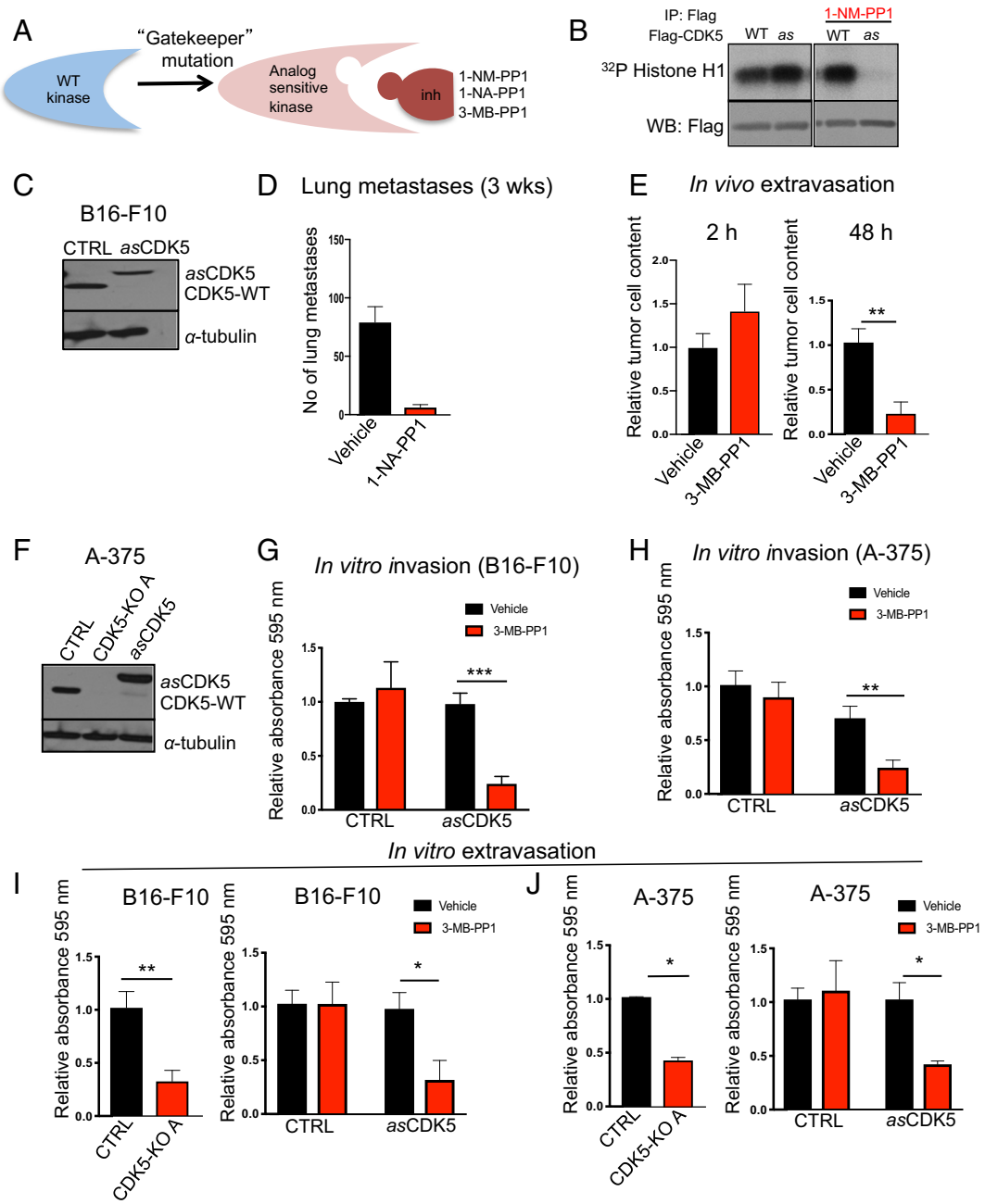

Fig. 4. The kinase activity of CDK5 is required for tumor cells extravasation. (*A*) Schematic representation of the analog-sensitive approach. (*B*) Flag-tagged wild-type (WT) or analog-sensitive (*as*) CDK5 were expressed in 293T cells, immunoprecipitated with an anti-Flag antibody and subjected to in vitro kinase reactions using histone H1 as a substrate (a canonical substrate of CDKs), in the presence of radioactive [γ^{32}P]-ATP and in the presence or absence of 5 μM 1-NM-PP1 (inhibitor of *as* kinases). Radiolabeled histone H1 was detected by autoradiography. Note that in the absence of 1-NM-PP1, wild-type and *as* CDK5 display comparable kinase activities. Addition of 1-NM-PP1 blocks the activity of *as* CDK5 without affecting wild-type CDK5. (*C*) Immunoblotting for CDK5 in mouse melanoma B16-F10 cells (CTRL), or B16-F10 cells in which we knocked out the endogenous CDK5 using CRISPR/Cas9 and expressed Flag-tagged *as* CDK5 (*as*CDK5). CDK5-WT, endogenous wild-type Cdk5. α-Tubulin was used as a loading control ($n = 2$). (*D*) The numbers of lung metastases in C57BL/6 mice injected with *as*CDK5 B16-F10 melanoma cells, quantified after 3 wk. Mice were treated with vehicle or with an inhibitor of *as* kinases 1-NA-PP1, from day 0 until the end of the experiment ($n = 5$ mice/group) (*SI Appendix, Materials and Methods*). Shown are mean values ± SD ***$P < 0.001$ (unpaired *t* test with Welch's correction). (*E*) Fluorescently labeled *as*CDK5 B16-F10 cells were injected into tail veins of *Foxn1*^{nu}. Recipient mice were treated with vehicle or with an inhibitor of *as* kinases 3-MB-PP1 ($n = 3$ mice/group). Lungs were imaged after 2 (*Left*) and 48 h (*Right*). Shown are mean values ± SD **$P < 0.01$ (unpaired *t* test). (*F*) Immunoblotting for CDK5 in human melanoma A-375 cells (CTRL), A-375 cells in which we knocked out the endogenous CDK5 using CRISPR/Cas9 (CDK5-KO A), and CDK5-KO cells in which we expressed Flag-tagged *as*CDK5 (*as*CDK5). α-Tubulin was used as a loading control ($n = 2$). (*G*) In vitro invasion assays. Parental mouse melanoma B16-F10 cells (CTRL) or B16-F10 cells engineered to express *as*CDK5 in place of wild-type CDK5 (*as*CDK5) were subjected to invasion assays in the presence of vehicle or 3-MB-PP1 ($n = 3$; in triplicate). Shown are mean values ± SD ***$P < 0.001$ (two-way ANOVA, Bonferroni's multiple comparisons test). (*H*) Similar assays as in *G*, using parental human melanoma A-375 cells (CTRL) or A-375 cells expressing *as*CDK5 ($n = 3$; in triplicate). Shown are mean values ± SD. **$P < 0.01$ (two-way ANOVA, Bonferroni's multiple comparisons test). (*I*) In vitro transendothelial migration (in vitro extravasation) assays using parental (CTRL) and CDK5-KO mouse melanoma B16-F10 cells (*Left*) ($n = 3$; in triplicate), or parental B16-F10 (CTRL) and *as*CDK5 B16-F10 cells (*as*CDK5) assayed in the presence of vehicle or 3-MB-PP1 (*Right*) ($n = 3$; in triplicate). (*J*) Similar assays as in *I*, using human melanoma A-375 cells ($n = 3$; in triplicate). In *I* and *J* data are shown as mean values ± SD **$P < 0.01$, *$P < 0.05$ (unpaired *t* test).

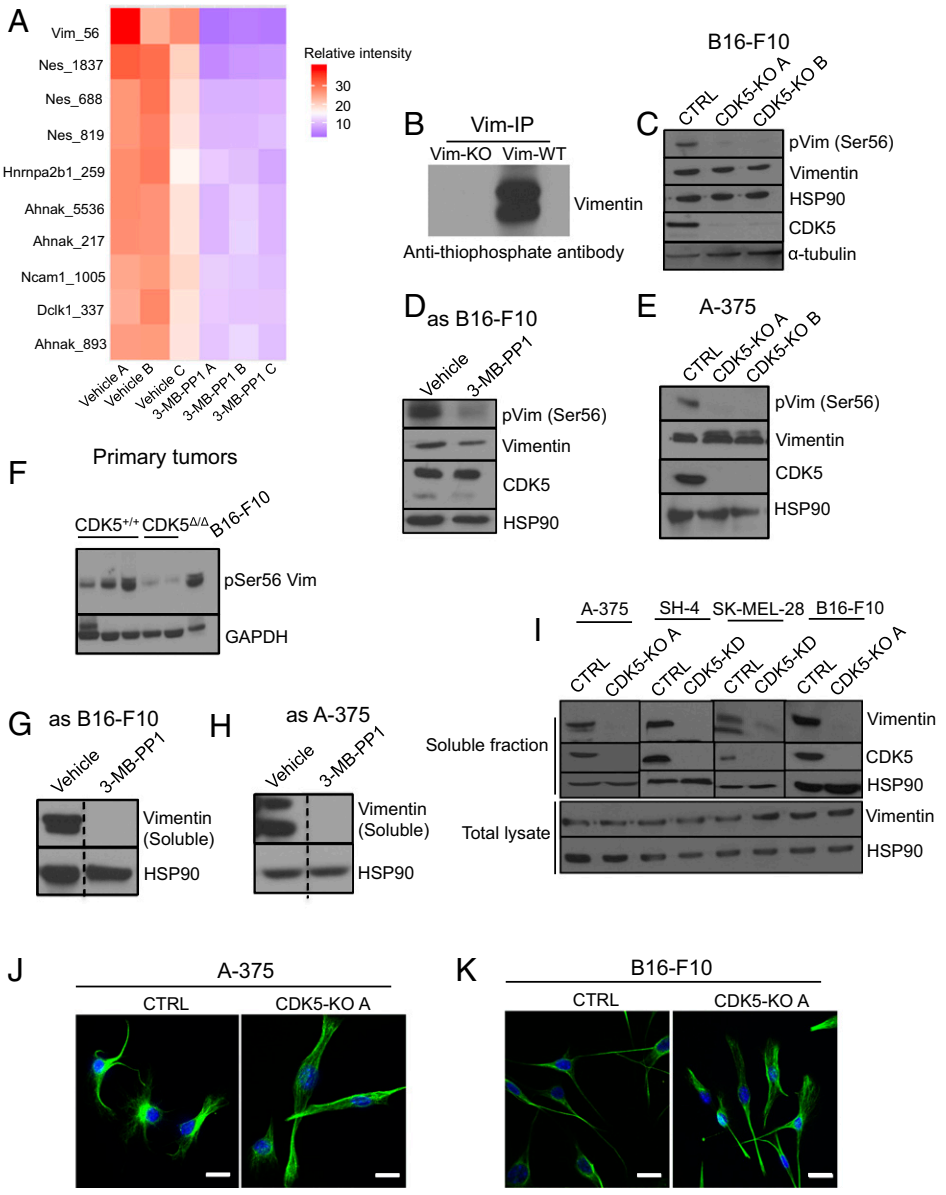

Fig. 5. CDK5 phosphorylates vimentin in melanoma cells and regulates its polymerization. (*A*) Heat map depicting 10 phosphosites (only S/T-P sequences are shown) which displayed the most strongly decreased phosphorylation upon CDK5 inhibition. Three independent cultures of vehicle-treated (vehicle A, B, and C) or 3-MB-PP1-treated (3-MB-PP1 A, B, and C) *as*CDK5 B16-F10 cells were analyzed. For each phosphopeptide, the intensities (abundance) across all six samples were scaled to 100, and the top 10 phosphorylated peptides displaying the highest fold decrease in phosphorylation levels in CDK5-inhibited samples were used to make the heat map. The relative abundance in each sample was color coded, as indicated. (*B*) In cell kinase reactions. In vitro cultured *as*CDK5 B16-F10 cells (Vim-WT) or, for control, vimentin knockout *as*CDK5 B16-F10 cells (Vim-KO) were permeabilized by treatment with 30 μg/mL digitonin and supplemented with N^6-substituted bulky ATP analog, N^6-furfuryl-ATPγS for 30 min, resulting in thio-phosphorylation of direct CDK5 substrates. Proteins were then alkylated with p-nitrobenzyl mesylate to generate epitopes for an anti-thiophosphate ester antibody. Endogenous vimentin was immunoprecipitated with an anti-vimentin antibody, and immunoblots were probed with an anti-thiophosphate ester antibody to evaluate thio-phosphorylation of vimentin. Please note the absence of signal for thio-phosphorylated vimentin in vimentin knockout *as*CDK5 B16-F10 cells (Vim-KO). (*C*) Protein lysates from $CDK5^{+/+}$ (CTRL) and CDK5-knockout (CDK5-KO A, CDK5-KO B; A and B denote different sgRNAs, see *SI Appendix, Materials and Methods*) B16-F10 cells were immunoblotted with antibodies against phospho-serine56-vimentin, total vimentin, or CDK5. HSP90 and α-tubulin were used as loading controls ($n = 3$). (*D*) Similar analysis as in *C*, using *as*CDK5 B16-F10 cells cultured for 4 h in the presence of vehicle or 3-MB-PP1 (to inhibit CDK5) ($n = 2$). (*E*) Similar analysis as in *C*, using parental (CTRL) and CDK5-KO human melanoma A-375 cells ($n = 2$). (*F*) Similar analysis as in *C*, using tumors arising in $CDK5^{+/+}$/Tyr-Cre/$BRAF^{V600E/+}$/$PTEN^{F/F}$ ($CDK5^{+/+}$) or $CDK5^{F/F}$/Tyr-Cre/$BRAF^{V600E/+}$/$PTEN^{F/F}$ ($CDK5^{\Delta/\Delta}$) mice. B16-F10 cells were used as a positive control. Immunoblotting for GAPDH was used as a loading control ($n = 2$). (*G*) *as*CDK5 mouse melanoma B16-F10 cells were cultured for 4 h in the presence of vehicle or 3-MB-PP1. Cells were lysed, the soluble fraction was obtained as described in *SI Appendix, Materials and Methods*, and immunoblotted with an anti-vimentin antibody. HSP90 served as a loading control ($n = 2$). The lines were spliced together from the same blot (indicated by dashed lines). (*H*) Similar analysis as in *G*, using *as*CDK5 human melanoma A-375 cells ($n = 2$). The lines were spliced together from the same blot (indicated by dashed lines). (*I*) *Upper* (soluble fraction) human (A-375, SH-4, SK-MEL-28), and mouse (B16-F10) melanoma cells: parental (CTRL), CDK5-KO, or cells in which we depleted CDK5 using anti-CDK5 shRNA (CDK5-KD), were lysed and the soluble fractions obtained as described in *SI Appendix, Materials and Methods*. Immunoblots were probed for vimentin, CDK5, and HSP90 (loading control). Extract from each melanoma cell line was run on a separate blot (indicated by solid vertical lines). *Lower* (total lysate) total cell lysates (containing soluble and insoluble proteins) were immunoblotted for vimentin and HSP90. (*J*) In vitro cultured parental (CTRL) and CDK5-KO human A-375 melanoma cells were immunostained using an anti-vimentin antibody and analyzed by confocal microscopy. Hoechst staining was used to visualize nuclei. (*K*) Similar analysis as in *J* with cultured parental (CTRL) and CDK5-KO mouse B16-F10 melanoma cells. (Scale bars, 50 μm.)

in vivo. To do so, we took advantage of the observation that analog-sensitive kinases can accept N^6-substituted bulky ATP analogs, while wild-type kinases cannot utilize these analogs, due to steric hindrance (44). Hence, by providing cells expressing an analog-sensitive kinase with bulky ATP analogs in which the gamma phosphate has been replaced with a thiophosphate moiety, one can uniquely label direct kinase substrates with a thiophosphate tag (44). This tag can be then used to identify substrate proteins (44).

We cultured *as*CDK5 B16-F10 melanoma in the presence of a bulky ATPγS analog (N^6-furfuryl-ATPγS), resulting in thiolabeling of direct CDK5 substrates. We then immunoprecipitated the endogenous vimentin and probed the immunoblots with an anti-thiophosphate ester antibody (to detect thio-phosphorylation). Using this approach, we confirmed that vimentin represents a direct substrate of CDK5 in vivo in melanoma cells (Fig. 5*B*). We also confirmed, using in vitro kinase reactions with purified, recombinant wild-type CDK5-p35 and vimentin, that vimentin represents a direct CDK5 phosphorylation substrate (*SI Appendix*, Fig. S5*B*). Using mass spectrometry we verified that CDK5 phosphorylates vimentin on serine 56 (Dataset S2). This residue conforms to the canonical serine/threonine–proline phosphorylation motif for CDK5 (6).

We next analyzed the phosphorylation status of serine 56 residue of the endogenous vimentin in melanoma cells, using an anti-phospho-serine 56-vimentin antibody. We observed that knockout of CDK5, or an acute inhibition of CDK5 kinase in mouse or human melanoma cells strongly decreased phosphorylation of this vimentin residue (Fig. 5 *C–E*). We also verified that CDK5-deleted autochthonous melanomas arising in $CDK5^{F/F}$/Tyr-Cre/$BRAF^{V600E/+}$/$PTEN^{F/F}$ mice showed strongly decreased vimentin serine 56 phosphorylation, as compared to melanomas in $CDK5^{+/+}$ mice (Fig. 5*F*). We concluded that in melanoma cells and tumors, the phosphorylation of vimentin serine 56 is regulated by CDK5.

Since phosphorylation of serine 56 of vimentin depolymerizes vimentin filaments (38, 39, 45), we quantified the relative amounts of depolymerized "soluble" vimentin and "insoluble" vimentin filaments in melanoma cells. To this end, we fractionated cell lysates into soluble and insoluble fractions and immunoblotted them with anti-vimentin antibodies. We observed that knockout of CDK5, or inhibition of CDK5 kinase, led to an essentially complete loss of soluble vimentin (Fig. 5 *G–I*). Consistent with these findings, immunostaining of in vitro cultured mouse and human melanoma cells revealed that ablation of CDK5 promoted formation of well-defined vimentin filaments (Fig. 5 *J* and *K*). Collectively, these findings suggest that in melanoma cells CDK5 maintains the pool of soluble vimentin, by directly phosphorylating this protein. Inhibition of CDK5, and the resulting loss of serine 56 phosphorylation of vimentin, triggers depletion of soluble vimentin, which becomes incorporated into vimentin filaments.

To test whether the loss of vimentin phosphorylation upon CDK5 inhibition is causally linked to decreased invasiveness of melanoma cells, we engineered CDK5 knockout mouse B16-F10 and human A-375 melanoma cells to express a vimentin mutant containing phosphomimicking serine to aspartic acid (S→D) substitution within vimentin's CDK5-dependent serine 56 residue (Fig. 6 *A* and *B*). We first analyzed the ability of these cells to invade in vitro, using Transwell assays. As expected, knockout of CDK5 impeded the invasiveness of mouse and human melanoma cells. Importantly, expression of phosphomimicking vimentin in CDK5-null cells largely restored the ability of these cells to invade in vitro (Fig. 6 *C* and *D*).

To extend these observations in vivo, we injected $CDK5^{+/+}$ (control), or CDK5-KO, or CDK5-KO melanoma cells expressing phosphomimicking vimentin, into tail veins of C57BL/6 mice and gauged the ability of melanoma cells to form lung metastases after 3 and 4 wk. As expected, $CDK5^{+/+}$ cells formed massive lung metastases. Also as predicted from our earlier analyses, ablation of CDK5 nearly extinguished the ability of melanoma cells to form metastases (Fig. 6 *E* and *F*). Strikingly, expression of phosphomimicking vimentin in CDK5-knockout cells fully restored the ability of CDK5-null cells to form metastases (Fig. 6 *E* and *F*). Hence, expression of phosphomimicking vimentin obviates the requirement for CDK5 in metastasis in vivo. We concluded that the ability of CDK5 to phosphorylate and depolymerize vimentin underlies the essential role for this kinase in promoting the invasiveness of melanoma cells. Inhibition of CDK5 strongly decreases vimentin Ser56 phosphorylation, diminishes the soluble vimentin pool, and triggers incorporation of vimentin into polymers, thereby inhibiting cell invasiveness.

Chemical Inhibition of CDK5 Impedes the Metastasis of Human Melanomas in PDX Models. Genetic ablation of CDK5, or highly selective inhibition of analog-sensitive CDK5 using *as* inhibitors cannot be utilized for therapeutic purposes. While no CDK5-specific inhibitors are currently available, several pan-CDK inhibitors, such as roscovitine, can inhibit CDK5 kinase activity (46, 47). For this reason, we asked whether treatment of melanoma cells with roscovitine would affect polymerization of vimentin. Indeed, as we observed upon CDK5 ablation, treatment of B16-F10 cells with roscovitine resulted in nearly complete loss of Ser56-phosphorylated and soluble vimentin (Fig. 7 *A* and *B* and *SI Appendix*, Fig. S6*A*). We extended these observations using a culture of patient-derived metastatic melanoma cells. Again, treatment of these cells with roscovitine greatly diminished the pool of soluble vimentin (Fig. 7*C*).

Encouraged by these results, we asked whether roscovitine treatment would block the metastatic spread of patient-derived melanomas in vivo. We utilized two mouse models of PDXs. The models were derived from breast (model WCM214) and lymph node (WND238) metastatic lesions (48, 49). Importantly, both models are highly metastatic in mice and rapidly spread to the lungs of the recipient animals. We subcutaneously implanted human tumors into recipient mice and started daily treatment of animals with roscovitine or with vehicle (control) as soon as tumors became palpable. At the end of the observation period, we collected the internal organs and analyzed them by histology. As expected, tumors in vehicle-treated animals spread to the lungs, where we detected numerous metastases. In contrast, treatment of tumor-bearing mice with roscovitine strongly decreased the metastatic burden (Fig.7 *D*, *E*, *G*, and *H*). Importantly, roscovitine treatment had only a very mild effect on the growth of primary tumors (Fig. 7 *F* and *I* and *SI Appendix*, Fig. S6 *B–E*). These observations indicate that inhibition of CDK5 might represent a very attractive therapeutic strategy to block the metastatic spread of melanoma cells.

Discussion

Work of the past decade has documented that CDK5-p35 kinase is activated in many different human tumor types, including pancreatic, lung, liver, breast, ovarian, prostate, and colorectal cancers (10, 11, 13, 14, 50, 51). However, the molecular function of the CDK5 kinase in tumor cells remains unclear.

The best documented is the ability of CDK5 to promote proliferation of tumor cells. It was reported that transgenic mice engineered to overexpress p25 (a hyperactive form of p35) in thyroid C cells developed medullary thyroid carcinoma (MTC) (52). Importantly, tumor cell proliferation was dependent on p25, as switching off p25 expression halted MTC tumor growth (52). At the molecular level, the authors found that in tumor cells, CDK5 phosphorylates and functionally inactivates the retinoblastoma protein (RB1), thereby driving cell proliferation (52, 53). Another group reported that in MTC cells CDK5 promotes tumor cell proliferation by phosphorylating a transcription factor STAT3 (54). Moreover, some groups concluded that CDK5 inhibits cell proliferation (55–57), while others postulated that CDK5 plays no role in tumor growth (51, 58). It should be noted that many of these studies (except for p25 transgenic mice) utilized dominant negative CDK5 constructs, or shRNAs, or pan-CDK inhibitors, which could result in off-target effects.

In addition to proliferation, several studies reported that CDK5 plays a role in regulating cancer cell motility. Depending on the study, CDK5 was shown to promote migration of cancer cells by phosphorylating actin-binding/regulatory proteins such as caldesmon, talin, or FAK, phosphatidylinositol 4-phosphate 5-kinase type I γ (PIPKIγ90), PIKE-A, a transcription factor USF2, or to indirectly activate small GTP-ases RalA and RalB (11, 50, 51, 58–63). In contrast, other authors concluded that CDK5 serves to inhibit cancer cell migration and to suppress metastasis by phosphorylating a tumor-suppressor DLC1, a scaffold protein muskelin, a transmembrane glycoprotein PDPN, an epigenetic regulator EZH2, or a protein phosphatase PP2A (64–68). Again, these studies mainly utilized nonspecific inhibitors, dominant-negative CDK5 constructs, or shRNAs. Lastly, CDK5 has been postulated to regulate other aspects of tumorigenesis, such as promoting or inhibiting survival, or DNA repair, or angiogenesis (14).

In this study we focused on the function of CDK5 in melanoma. Malignant melanoma is the deadliest form of skin cancer, due to its aggressive clinical behavior and the ability to form metastases. Melanoma is responsible for over 50,000 deaths per year worldwide, and nearly all of them are caused by the metastatic spread (69, 70). We decided to evaluate the function of CDK5 in melanoma using genetic means, namely mice that

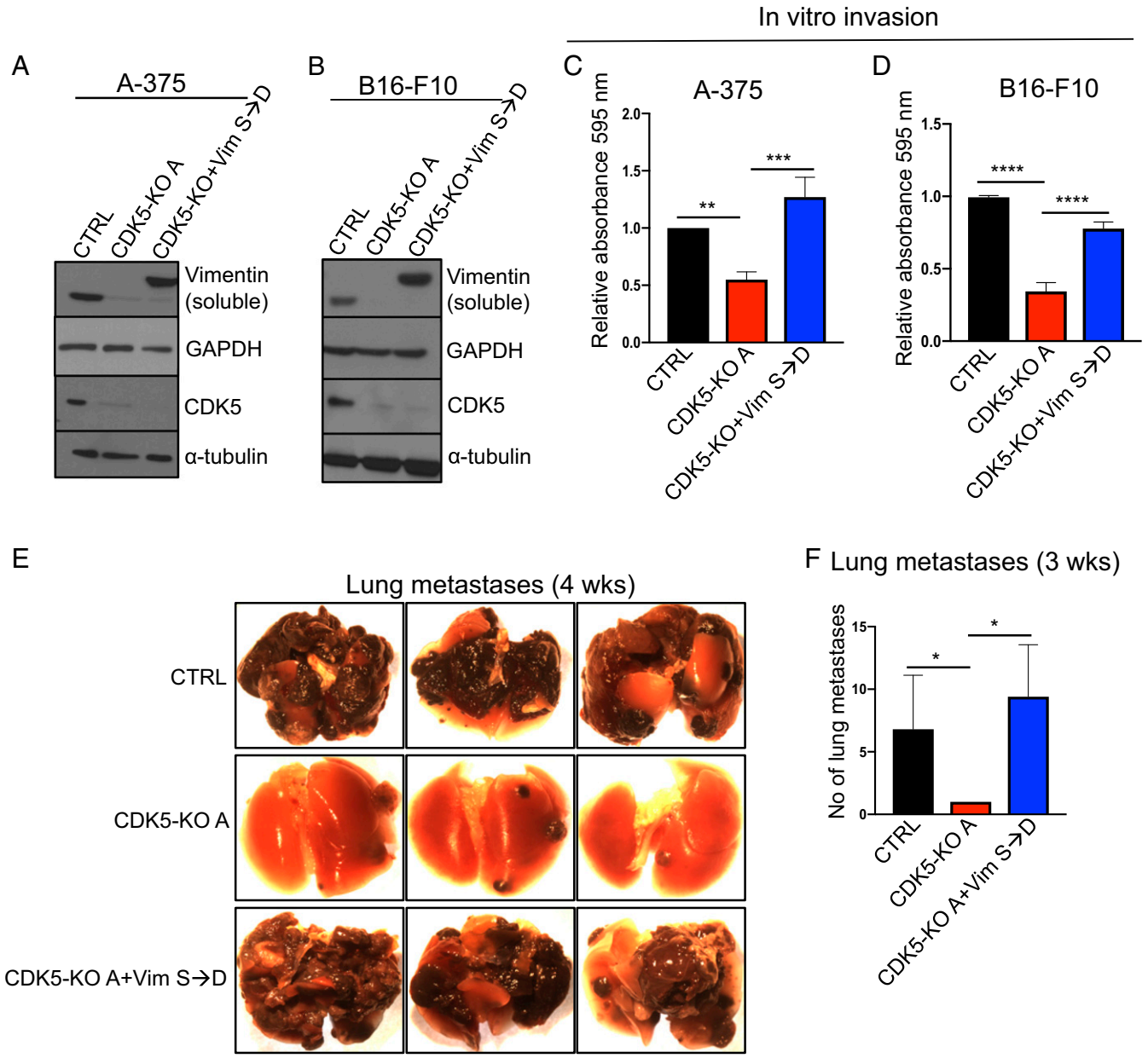

Fig. 6. Rescue of the invasion defect in CDK5-null cells by phosphomimicking vimentin. (*A*) Parental (CTRL), CDK5-KO, and CDK5-KO cells expressing Flag-tagged vimentin phosphomimicking mutant containing serine 56 to aspartic acid substitution (Vim S→D) human melanoma A-375 cells were lysed to obtain soluble protein fractions. Immunoblots were probed for vimentin and CDK5. GAPDH and α-tubulin were used as loading controls ($n = 2$). (*B*) Similar analysis as in *A* using mouse melanoma B16-F10 cells ($n = 2$). (*C*) In vitro invasion assays using parental human melanoma A-375 cells (CTRL), A-375 CDK5-KO cells, or CDK5-KO cells expressing S56D phosphomimicking vimentin (CDK5-KO+VimS→D, from *A*) ($n = 3$; in triplicate). Shown are mean values ± SD $^{**}P < 0.01$, $^{***}P < 0.001$ (one-way ANOVA with Tukey's multiple comparisons test). (*D*) Similar assays as in *C*, using parental mouse B16-F10 melanoma cells (CTRL), or B16-F10 CDK5-KO cells, or CDK5-KO cells expressing S56D phosphomimicking vimentin (CDK5-KO+VimS→D, from *B*) ($n = 3$; in triplicate). Shown are mean values ± SD $^{****}P < 0.0001$ (one-way ANOVA with Tukey's multiple comparisons test). (*E*) Parental mouse melanoma B16-F10 cells (CTRL), or CDK5 knockout B16-F10 cells (CDK5-KO), or CDK5-KO cells expressing phosphomimicking S56D vimentin (CDK5-KO+VimS→D) were injected into tail veins of C57BL/6 mice ($n = 5$ mice/group). Animals were euthanized and lungs photographed after 4 wk. (*F*) Similar experiment as in *E*, the numbers of lung metastases were quantified after 3 wk ($n = 5$ mice/group). Shown are mean values ± SD $^{*}P < 0.05$ (Kruskal-Wallis test with Dunn's multiple comparisons test).

allow specific ablation of CDK5 in autochthonous tumors. We also engineered mouse and human melanoma cells to express analog-sensitive CDK5 in place of wild-type CDK5. These cells allowed a highly selective inhibition of CDK5 kinase in tumor cells. Lastly, we utilized cell cultures derived directly from human melanomas as well as PDX of human melanomas. All these analyses revealed that CDK5 is dispensable for tumor cell proliferation, but it is essential for the metastatic spread, as ablation or inhibition of CDK5 halted the metastasis.

Our results are consistent with the study of Bisht et al. (61), who reported that shRNA-mediated depletion of CDK5 inhibited the invasiveness of melanoma cells in vitro as well as metastasis in vivo. These authors also observed that depletion of CDK5 inhibited the growth of primary tumors derived from a xenografted human melanoma cell line (61). In contrast, we found that a genetic ablation of CDK5 had no impact on proliferation of autochthonous primary mouse melanomas. Likewise, we found that inhibition of CDK5

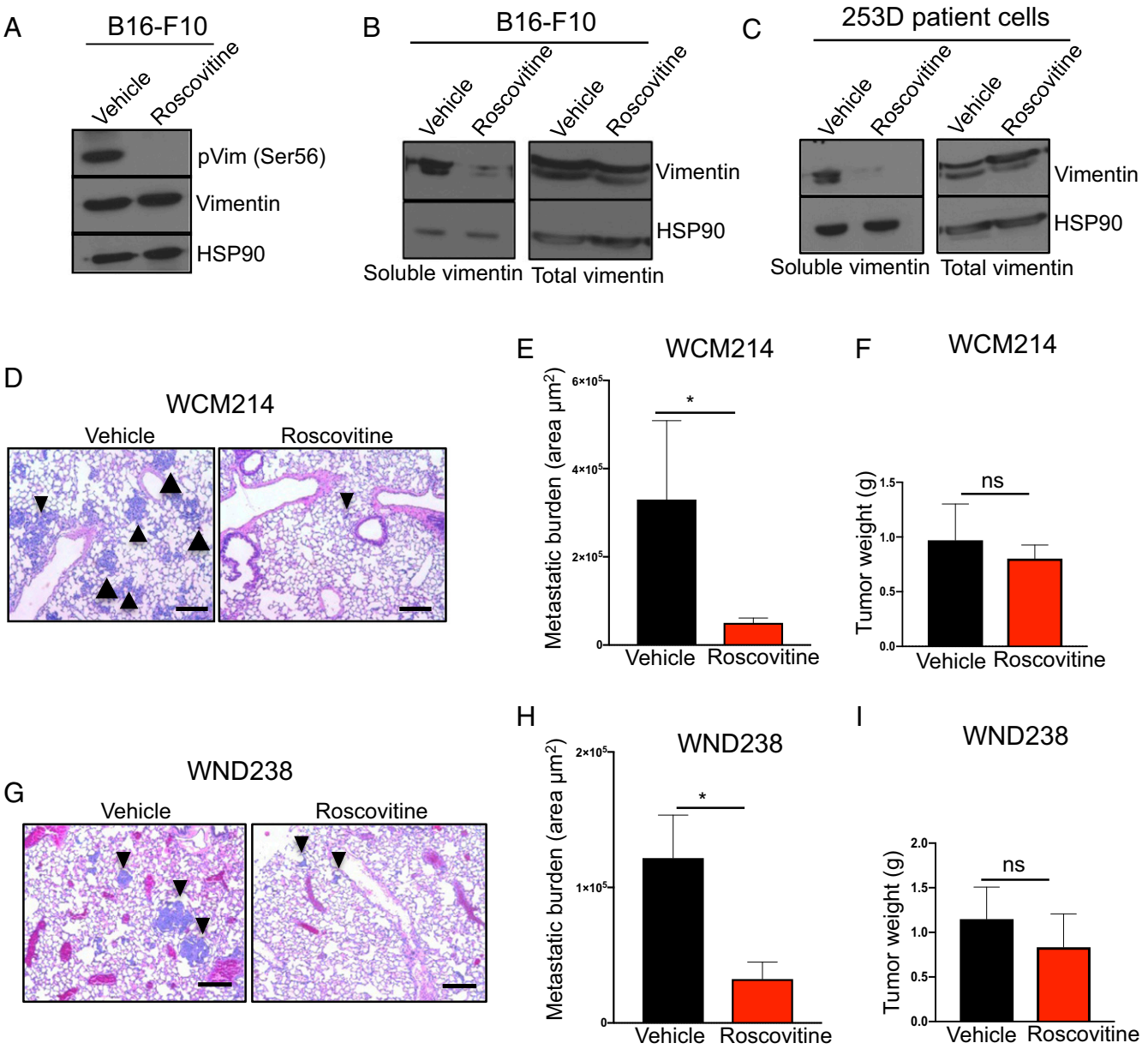

Fig. 7. CDK5 inhibition in melanoma cells and patient-derived xenografts. (*A*) Mouse B16-F10 cells were cultured in the presence of vehicle or 5 μM roscovitine for 4 h, lysed, and immunoblotted with antibodies against phospho-serine56-vimentin and total vimentin. HSP90 was used as a loading control ($n = 2$). (*B*) B16-F10 cells were cultured as above. *Left* (soluble vimentin), cells were lysed and the soluble fraction obtained as described in *SI Appendix, Materials and Methods*. Immunoblots were probed for vimentin and HSP90 (loading control). *Right* (total vimentin), total lysates (containing soluble and insoluble fractions) were also immunoblotted as above. (*C*) Patient-derived melanoma cells (253D) were cultured in the presence of vehicle or 5 μM roscovitine for 4 h, and analyzed as in *B* for the presence of soluble and total vimentin. (*D*) Histological sections of lungs from mice implanted with patient-derived melanoma tumors (model WCM214). Mice were treated with roscovitine (daily i.p. injection, 150 mg/kg) or with vehicle for 28 d ($n = 10$ mice/group; see *SI Appendix, Materials and Methods*). Arrowheads point to examples of metastases. (Scale bars, 50 μm.) (*E*) Total metastatic burden in mice implanted with patient-derived melanoma tumors (model WCM214). Mice were treated as above with vehicle or roscovitine, euthanized, and their internal organs subjected to histopathological analyses for the presence of metastases. Only lung metastases were detected. To estimate total metastatic burden in a given animal, the total area occupied by metastases was calculated in step sections of lungs ($n = 5$ mice/group; see *SI Appendix, Materials and Methods*). (*F*) The total weight of primary tumors in mice implanted with patient-derived melanomas (model WCM214) at the end of treatment. Mice were treated as above with vehicle or roscovitine, euthanized after 28 d, and tumors were weighted ($n = 10$ mice/group). (*G*) Similar analysis as in *D* in mice bearing xenografts of patient-melanoma tumors (model WND238). Mice were treated with vehicle or roscovitine for 49 d ($n = 10$ mice/group). (Scale bars, 50 μm.) (*H*) Similar analysis as in *E* in mice bearing xenografts of patient-melanoma tumors (model WND238) ($n = 10$ mice/group). Mice were treated with vehicle or roscovitine for 49 d. (*I*) Similar analysis as in *F* in mice bearing xenografts of patient-melanoma tumors (model WND238). Shown in *E*, *F*, *H*, and *I* are mean values ± SE $*P < 0.05$ (Mann–Whitney *U* test). ns, not significant.

kinase after the extravasation had been completed did not impede the growth of lung tumors. Lastly, treatment of mice bearing patient-derived xenografts with roscovitine had only a small impact of primary tumors, but it strongly impeded the metastasis.

It may not be surprising that CDK5 is not needed for proliferation of melanoma cells, at least in our systems. In most cell types, the phosphorylation of RB1 is carried out by the D-type cyclins acting together with CDK4 and CDK6, as well as E-cyclins and CDK2 (1, 2). In a large fraction of malignant

tumors, these cyclins are overexpressed and/or hyperactivated, resulting in a constitutive phosphorylation and inactivation of RB1 (5, 71). This is clearly the case in the majority of melanomas, which contain deletion of the *CDKN2A* gene encoding an inhibitor of cyclin D-CDK4/6, $p16^{INK4a}$ (19). Loss of $p16^{INK4a}$ causes hyperactivation of cyclin D-CDK4/6 kinases, resulting in constitutive phosphorylation of RB1 (5, 17). While the melanoma mouse model used in our study expresses wild-type *CDKN2A*, the oncogenically activated $BRAF^{V600E}$ allele stimulates the MAPK pathway, which transcriptionally up-regulates cyclin D1, resulting in an increased activity of cyclin D-CDK4/6 kinase (17, 72, 73). Hence, all these lesions obviate the need for additional kinases, such as CDK5, in phosphorylating RB1. It is possible that in several MTC cases the levels of cyclin D-CDK4/6 and E-CDK2 are low, and in this setting overexpressed CDK5 may contribute to RB1 inactivation, as reported by Pozo et al. (52).

Our mechanistic analyses revealed that CDK5 regulates melanoma cell invasiveness by directly phosphorylating vimentin. Several lines of evidence support this model: 1) We demonstrated, using human melanoma cells expressing analog-sensitive CDK5 and the thio-labeling approach that CDK5 directly phosphorylates the endogenous vimentin in melanoma cells. 2) CDK5 plays an essential, rate-limiting role in regulating phosphorylation status of vimentin in melanoma cells, as revealed by our unbiased, proteomewide analyses. 3) We documented strongly decreased phosphorylation of the endogenous vimentin and the concomitant loss of soluble vimentin upon CDK5 ablation or CDK5 kinase inhibition in three human melanoma cell lines, in a culture of patient-derived tumor cells, in a mouse melanoma cell line, as well as in autochthonous tumors arising in Tyr-Cre/$BRAF^{V600E/+}$/$PTEN^{F/F}$ mice. 4) Expression of a vimentin mutant containing a phosphomimicking substitution within the CDK5-dependent phospho-residue bypassed the requirement for CDK5 in melanoma metastasis and fully restored the metastatic potential of CDK5-null cells. It should be noted that CDK5 was previously reported to phosphorylate vimentin in neutrophil granulocytes and to regulate GTP-induced secretion via this mechanism (74). Hence, this molecular mechanism may be used in different cell types to regulate distinct cellular functions.

The role of vimentin in promoting cell motility has been well documented. For example, vimentin plays a rate-limiting function in regulating transendothelial migration of leukocytes (75). Phosphorylation of vimentin, and the resulting disassembly of vimentin filaments was shown to play an important role in promoting cell migration (36, 40). Hence, it is likely that also in other tumor types which express vimentin, CDK5 may promote cell invasiveness by directly phosphorylating vimentin. Alternatively, in different cancer types CDK5 may regulate tumor cell motility by phosphorylating other proteins involved in migration. In neurons, a cell type in which the rate-limiting role of CDK5 in regulating migration has been best documented (76, 77), phosphorylation of several proteins has been proposed to underlie this function. Most of the implicated proteins play a role in regulating organization and function of microtubules or actin filaments (8). It is hence possible that in addition to vimentin, CDK5 may regulate other cytoskeletal proteins in other types of tumors. It is also plausible that CDK5 regulates different functions (such as migration or proliferation), depending on tumor type. Additional studies of other cancer types utilizing genetic and chemical-genetic means (such as the analog-sensitive approach) will help to resolve these issues.

In agreement with our analyses of the mouse genetic model, we found that treatment of mice bearing highly metastatic patient-derived melanomas with roscovitine strongly inhibited the metastatic dissemination, while having little effect on the growth of primary tumors. Collectively, our results indicate that inhibition of CDK5 kinase might represent a very attractive therapeutic strategy to block the metastatic spread of tumor cells.

Our study highlights the need for developing more potent and specific CDK5 inhibitors. Since no such inhibitors are currently available, in our PDX experiments we used roscovitine, which represents a pan-CDK inhibitor. Another "CDK5-specific" inhibitor, *N*-(5-isopropylthiazol-2-yl)-3-phenylpropanamide (PJB), used for in vitro studies, also inhibits CDK2 (61). Potent and selective CDK5 inhibitors will likely have an even stronger effect on tumor dissemination and might very efficiently block the metastatic spread, as seen upon genetic CDK5 ablation. The enthusiasm for using CDK5 inhibitors in cancer treatment may be mitigated by the observation that CDK5 is active in postmitotic neurons (6, 8). Hence, one must also consider the consequences of CDK5 inhibition for the physiology of the nervous system. However, while CDK5 is essential for the development of the nervous system (76, 77), the consequences of CDK5 inhibition in an adult organism are likely much milder. For example an acute CDK5 knockout in the adult mouse brain had only very limited consequences, and it actually increased synaptic plasticity and learning ability (78). Given that the metastatic spread—not the primary tumors—are responsible for the lion's share of cancer-related mortality, we propose that CDK5 inhibition might represent a potent therapeutic strategy, in conjunction with modalities that target the primary tumor.

Materials and Methods

Mice. For analyses of the melanoma mouse model, $BRaf^{CA}$, $Pten^{loxP}$, Tyr::$CreER^{T2}$ mice (further referred to as Tyr-Cre/$BRAF^{V600E/+}$/$PTEN^{F/F}$) were crossed with $Cdk5^{tm1.1Lht}$ ($CDK5^{F/F}$) mice (both strains from The Jackson Laboratory) to generate experimental $CDK5^{F/F}$/Tyr-Cre/$BRAF^{V600E/+}$/$PTEN^{F/F}$ and control $CDK5^{+/+}$/Tyr-Cre/$BRAF^{V600E/+}$/$PTEN^{F/F}$ animals. Both male and female neonates were used for the experiments. Experiments involving tail vein injections of B16-F10 cells were performed using 7-wk-old female C57BL/6 mice (The Jackson Laboratory), except for the experiments shown in Figs. 3*G* and 4*E* and *SI Appendix*, Fig. S3 *D* and *E*), in which 7-wk-old female $Foxn1^{nu}$ mice (The Jackson Laboratory) were used. All animals were held in the same animal room in individually ventilated cages with a 12-h day/night cycle. All procedures were carried out according to the protocol approved by the Institutional Animal Care and Use Committee of the Dana-Farber Cancer Institute. All PDX experiments were performed at the Wistar Institute in accordance with the guidelines of the Wistar Institute's Institutional Animal Care and Use Committee (79). As the recipients of xenografts, 3- to 5-mo-old NSG male mice (The Jackson Laboratory) were used.

Data Availability. All data files, including additional materials and methods and associated protocols, are available in *SI Appendix*.

ACKNOWLEDGMENTS. This work was supported by grants from the National Cancer Institute R01CA239660 and R01CA202634 (to P.S.). We thank Drs. Dylan Fingerman and Alessandra Martorella for help with PDX experiments, Dr. Tobias Otto for help with statistical analyses, and Caitlin Mae Sullivan for help with the mouse colony.

1. M. Malumbres, Cyclin-dependent kinases. *Genome Biol.* **15**, 122 (2014).
2. S. Lim, P. Kaldis, Cdks, cyclins and CKIs: Roles beyond cell cycle regulation. *Development* **140**, 3079–3093 (2013).
3. M. Malumbres, M. Barbacid, Cell cycle, CDKs and cancer: A changing paradigm. *Nat. Rev. Cancer* **9**, 153–166 (2009).
4. C. J. Sherr, D. Beach, G. I. Shapiro, Targeting CDK4 and CDK6: From discovery to therapy. *Cancer Discov.* **6**, 353–367 (2016)
5. T. Otto, P. Sicinski, Cell cycle proteins as promising targets in cancer therapy. *Nat. Rev. Cancer* **17**, 93–115 (2017).
6. R. Dhavan, L. H. Tsai, A decade of CDK5. *Nat. Rev. Mol. Cell Biol.* **2**, 749–759 (2001).
7. L. H. Tsai, T. Takahashi, V. S. Caviness, Jr, E. Harlow, Activity and expression pattern of cyclin-dependent kinase 5 in the embryonic mouse nervous system. *Development* **119**, 1029–1040 (1993).
8. T. Kawauchi, Cdk5 regulates multiple cellular events in neural development, function and disease. *Dev. Growth Differ.* **56**, 335–348 (2014).
9. J. L. Liu *et al.*, Expression of CDK5/p35 in resected patients with non-small cell lung cancer: Relation to prognosis. *Med. Oncol.* **28**, 673–678 (2011).
10. R. Zhang *et al.*, Clinical role and biological function of CDK5 in hepatocellular carcinoma: A study based on immunohistochemistry, RNA-seq and *in vitro* investigation. *Oncotarget* **8**, 108333–108354 (2017).
11. J. P. Eggers *et al.*, Cyclin-dependent kinase 5 is amplified and overexpressed in pancreatic cancer and activated by mutant K-Ras. *Clin. Cancer Res.* **17**, 6140–6150 (2011).
12. W. W. Lockwood *et al.*, DNA amplification is a ubiquitous mechanism of oncogene activation in lung and other cancers. *Oncogene* **27**, 4615–4624 (2008).

13. K. Wei *et al*., An immunohistochemical study of cyclin-dependent kinase 5 (CDK5) expression in non-small cell lung cancer (NSCLC) and small cell lung cancer (SCLC): A possible prognostic biomarker. *World J. Surg. Oncol.* **14**, 34 (2016).
14. K. Pozo, J. A. Bibb, The emerging role of Cdk5 in cancer. *Trends Cancer* **2**, 606–618 (2016).
15. D. Dankort *et al*., Braf(V600E) cooperates with Pten loss to induce metastatic melanoma. *Nat. Genet.* **41**, 544–552 (2009).
16. W. E. Damsky *et al*., β-catenin signaling controls metastasis in Braf-activated Pten-deficient melanomas. *Cancer Cell* **20**, 741–754 (2011).
17. L. Chin, The genetics of malignant melanoma: Lessons from mouse and man. *Nat. Rev. Cancer* **3**, 559–570 (2003).
18. V. C. Gray-Schopfer, S. da Rocha Dias, R. Marais, The role of B-RAF in melanoma. *Cancer Metastasis Rev.* **24**, 165–183 (2005).
19. E. Hodis *et al*., A landscape of driver mutations in melanoma. *Cell* **150**, 251–263 (2012).
20. B. A. Samuels *et al*., Cdk5 promotes synaptogenesis by regulating the subcellular distribution of the MAGUK family member CASK. *Neuron* **56**, 823–837 (2007).
21. A. J. Cochran, D. R. Wen, S-100 protein as a marker for melanocytic and other tumours. *Pathology* **17**, 340–345 (1985).
22. C. L. Eberting, D. P. Shrayer, J. Butmarc, V. Falanga, Histologic progression of B16 F10 metastatic melanoma in C57BL/6 mice over a six week time period: Distant metastases before local growth. *J. Dermatol.* **31**, 299–304 (2004).
23. R. Ferretti, A. Bhutkar, M. C. McNamara, J. A. Lees, BMI1 induces an invasive signature in melanoma that promotes metastasis and chemoresistance. *Genes Dev.* **30**, 18–33 (2016).
24. R. D. Dorand *et al*., Cdk5 disruption attenuates tumor PD-L1 expression and promotes antitumor immunity. *Science* **353**, 399–403 (2016).
25. A. C. Bishop *et al*., A chemical switch for inhibitor-sensitive alleles of any protein kinase. *Nature* **407**, 395–401 (2000).
26. J. D. Blethrow, J. S. Glavy, D. O. Morgan, K. M. Shokat, Covalent capture of kinase-specific phosphopeptides reveals Cdk1-cyclin B substrates. *Proc. Natl. Acad. Sci. U.S.A.* **105**, 1442–1447 (2008).
27. K. Shah, Y. Liu, C. Deirmengian, K. M. Shokat, Engineering unnatural nucleotide specificity for Rous sarcoma virus tyrosine kinase to uniquely label its direct substrates. *Proc. Natl. Acad. Sci. U.S.A.* **94**, 3565–3570 (1997).
28. L. A. Witucki *et al*., Mutant tyrosine kinases with unnatural nucleotide specificity retain the structure and phospho-acceptor specificity of the wild-type enzyme. *Chem. Biol.* **9**, 25–33 (2002).
29. A. C. Bishop *et al*., Design of allele-specific inhibitors to probe protein kinase signaling. *Curr. Biol.* **8**, 257–266 (1998).
30. P. Mehlen, A. Puisieux, Metastasis: A question of life or death. *Nat. Rev. Cancer* **6**, 449–458 (2006).
31. G. C. McAlister *et al*., Increasing the multiplexing capacity of TMTs using reporter ion isotopologues with isobaric masses. *Anal. Chem.* **84**, 7469–7478 (2012).
32. M. Wühr *et al*., Accurate multiplexed proteomics at the MS2 level using the complement reporter ion cluster. *Anal. Chem.* **84**, 9214–9221 (2012).
33. A. Satelli, S. Li, Vimentin in cancer and its potential as a molecular target for cancer therapy. *Cell. Mol. Life Sci.* **68**, 3033–3046 (2011).
34. W. Wang *et al*., Vimentin is a crucial target for anti-metastasis therapy of nasopharyngeal carcinoma. *Mol. Cell. Biochem.* **438**, 47–57 (2018).
35. M. I. Rodríguez *et al*., PARP-1 regulates metastatic melanoma through modulation of vimentin-induced malignant transformation. *PLoS Genet.* **9**, e1003531 (2013).
36. J. Ivaska, H. M. Pallari, J. Nevo, J. E. Eriksson, Novel functions of vimentin in cell adhesion, migration, and signaling. *Exp. Cell Res.* **313**, 2050–2062 (2007).
37. Y. H. Chou, K. L. Ngai, R. Goldman, The regulation of intermediate filament reorganization in mitosis. p34cdc2 phosphorylates vimentin at a unique N-terminal site. *J. Biol. Chem.* **266**, 7325–7328 (1991).
38. Y. H. Chou, E. Rosevear, R. D. Goldman, Phosphorylation and disassembly of intermediate filaments in mitotic cells. *Proc. Natl. Acad. Sci. U.S.A.* **86**, 1885–1889 (1989).
39. Y. H. Chou, J. R. Bischoff, D. Beach, R. D. Goldman, Intermediate filament reorganization during mitosis is mediated by p34cdc2 phosphorylation of vimentin. *Cell* **62**, 1063–1071 (1990).
40. R. K. Sihag, M. Inagaki, T. Yamaguchi, T. B. Shea, H. C. Pant, Role of phosphorylation on the structural dynamics and function of types III and IV intermediate filaments. *Exp. Cell Res.* **313**, 2098–2109 (2007).
41. M. Inagaki, Y. Nishi, K. Nishizawa, M. Matsuyama, C. Sato, Site-specific phosphorylation induces disassembly of vimentin filaments in vitro. *Nature* **328**, 649–652 (1987).
42. M. Inagaki *et al*., Intermediate filament reconstitution in vitro. The role of phosphorylation on the assembly-disassembly of desmin. *J. Biol. Chem.* **263**, 5970–5978 (1988).
43. J. E. Eriksson *et al*., Specific in vivo phosphorylation sites determine the assembly dynamics of vimentin intermediate filaments. *J. Cell Sci.* **117**, 919–932 (2004).
44. N. T. Hertz *et al*., Chemical genetic approach for kinase-substrate mapping by covalent capture of thiophosphopeptides and analysis by mass spectrometry. *Curr. Protoc. Chem. Biol.* **2**, 15–36 (2010).
45. L. Cogli, C. Progida, R. Bramato, C. Bucci, Vimentin phosphorylation and assembly are regulated by the small GTPase Rab7a. *Biochim. Biophys. Acta* **1833**, 1283–1293 (2013).
46. G. N. Patrick, P. Zhou, Y. T. Kwon, P. M. Howley, L. H. Tsai, p35, the neuronal-specific activator of cyclin-dependent kinase 5 (Cdk5) is degraded by the ubiquitin-proteasome pathway. *J. Biol. Chem.* **273**, 24057–24064 (1998).
47. L. Meijer *et al*., Biochemical and cellular effects of roscovitine, a potent and selective inhibitor of the cyclin-dependent kinases cdc2, cdk2 and cdk5. *Eur. J. Biochem.* **243**, 527–536 (1997).
48. C. Krepler *et al*., A comprehensive patient-derived xenograft collection representing the heterogeneity of melanoma. *Cell Rep.* **21**, 1953–1967 (2017).
49. B. Garman *et al*., Genetic and genomic characterization of 462 melanoma patient-derived xenografts, tumor biopsies, and cell lines. *Cell Rep.* **21**, 1936–1952 (2017).
50. Q. Liang *et al*., CDK5 is essential for TGF-β1-induced epithelial-mesenchymal transition and breast cancer progression. *Sci. Rep.* **3**, 2932 (2013).
51. C. J. Strock *et al*., Cyclin-dependent kinase 5 activity controls cell motility and metastatic potential of prostate cancer cells. *Cancer Res.* **66**, 7509–7515 (2006).
52. K. Pozo *et al*., The role of Cdk5 in neuroendocrine thyroid cancer. *Cancer Cell* **24**, 499–511 (2013).
53. K. Pozo *et al*., Differential expression of cell cycle regulators in CDK5-dependent medullary thyroid carcinoma tumorigenesis. *Oncotarget* **6**, 12080–12093 (2015).
54. H. Lin, M. C. Chen, C. Y. Chiu, Y. M. Song, S. Y. Lin, Cdk5 regulates STAT3 activation and cell proliferation in medullary thyroid carcinoma cells. *J. Biol. Chem.* **282**, 2776–2784 (2007).
55. Y. Q. Sun *et al*., Low expression of CDK5 and p27 are associated with poor prognosis in patients with gastric cancer. *J. Cancer* **7**, 1049–1056 (2016).
56. A. K. Ajay *et al*., Cdk5 phosphorylates non-genotoxically overexpressed p53 following inhibition of PP2A to induce cell cycle arrest/apoptosis and inhibits tumor progression. *Mol. Cancer* **9**, 204 (2010).
57. L. Cao *et al*., Cyclin-dependent kinase 5 decreases in gastric cancer and its nuclear accumulation suppresses gastric tumorigenesis. *Clin. Cancer Res.* **21**, 1419–1428 (2015).
58. G. Feldmann *et al*., Inhibiting the cyclin-dependent kinase CDK5 blocks pancreatic cancer formation and progression through the suppression of Ras-Ral signaling. *Cancer Res.* **70**, 4460–4469 (2010).
59. C. Huang *et al*., Talin phosphorylation by Cdk5 regulates Smurf1-mediated talin head ubiquitylation and cell migration. *Nat. Cell Biol.* **11**, 624–630 (2009).
60. R. Liu *et al*., Cdk5-mediated regulation of the PIKE-A-Akt pathway and glioblastoma cell invasion. *Proc. Natl. Acad. Sci. U.S.A.* **105**, 7570–7575 (2008).
61. S. Bisht *et al*., Cyclin-dependent kinase 5 (CDK5) controls melanoma cell motility, invasiveness, and metastatic spread-identification of a promising novel therapeutic target. *Transl. Oncol.* **8**, 295–307 (2015).
62. L. Li *et al*., Cdk5-mediated phosphorylation regulates phosphatidylinositol 4-phosphate 5-kinase type I gamma 90 activity and cell invasion. *FASEB J.* **33**, 631–642 (2019).
63. T. F. Chi, T. Horbach, C. Götz, T. Kietzmann, E. Y. Dimova, Cyclin-dependent kinase 5 (CDK5)-mediated phosphorylation of upstream stimulatory factor 2 (USF2) contributes to carcinogenesis. *Cancers* **11**, E523 (2019).
64. H. Krishnan *et al*., PKA and CDK5 can phosphorylate specific serines on the intracellular domain of podoplanin (PDPN) to inhibit cell motility. *Exp. Cell Res.* **335**, 115–122 (2015).
65. B. K. Tripathi, D. R. Lowy, P. S. Zelenka, The Cdk5 activator P39 specifically links muskelin to myosin II and regulates stress fiber formation and actin organization in lens. *Exp. Cell Res.* **330**, 186–198 (2015).
66. B. K. Tripathi *et al*., CDK5 is a major regulator of the tumor suppressor DLC1. *J. Cell Biol.* **207**, 627–642 (2014).
67. X. Jin *et al*., CDK5/FBW7-dependent ubiquitination and degradation of EZH2 inhibits pancreatic cancer cell migration and invasion. *J. Biol. Chem.* **292**, 6269–6280 (2017).
68. J. Lu *et al*., CDK5 suppresses the metastasis of gastric cancer cells by interacting with and regulating PP2A. *Oncol. Rep.* **41**, 779–788 (2019).
69. I. Bedrosian *et al*., Incidence of sentinel node metastasis in patients with thin primary melanoma (< or = 1 mm) with vertical growth phase. *Ann. Surg. Oncol.* **7**, 262–267 (2000).
70. P. Corrie, M. Hategan, K. Fife, C. Parkinson, Management of melanoma. *Br. Med. Bull.* **111**, 149–162 (2014).
71. E. S. Knudsen, S. C. Pruitt, P. A. Hershberger, A. K. Witkiewicz, D. W. Goodrich, Cell cycle and beyond: Exploiting new RB1 controlled mechanisms for cancer therapy. *Trends Cancer* **5**, 308–324 (2019).
72. J. N. Lavoie, G. L'Allemain, A. Brunet, R. Müller, J. Pouysségur, Cyclin D1 expression is regulated positively by the p42/p44MAPK and negatively by the p38/HOGMAPK pathway. *J. Biol. Chem.* **271**, 20608–20616 (1996).
73. C. Albanese *et al*., Transforming p21ras mutants and c-Ets-2 activate the cyclin D1 promoter through distinguishable regions. *J. Biol. Chem.* **270**, 23589–23597 (1995).
74. K. Y. Lee, L. Liu, Y. Jin, S. B. Fu, J. L. Rosales, Cdk5 mediates vimentin Ser56 phosphorylation during GTP-induced secretion by neutrophils. *J. Cell. Physiol.* **227**, 739–750 (2012).
75. M. Nieminen *et al*., Vimentin function in lymphocyte adhesion and transcellular migration. *Nat. Cell Biol.* **8**, 156–162 (2006).
76. T. Ohshima *et al*., Targeted disruption of the cyclin-dependent kinase 5 gene results in abnormal corticogenesis, neuronal pathology and perinatal death. *Proc. Natl. Acad. Sci. U.S.A.* **93**, 11173–11178 (1996).
77. J. Ko *et al*., p35 and p39 are essential for cyclin-dependent kinase 5 function during neurodevelopment. *J. Neurosci.* **21**, 6758–6771 (2001).
78. A. H. Hawasli *et al*., Cyclin-dependent kinase 5 governs learning and synaptic plasticity via control of NMDAR degradation. *Nat. Neurosci.* **10**, 880–886 (2007).
79. W. Underwood, R. Anthony, S. Gwaltney-Brant, A. S. P. C. A. Poison, R. Meyer, *AVMA Guidelines for the Euthanasia of Animals* (American Veterinary Medical Association, IL, 2013).